Available online at www.sciencedirect.com

SCIENCE DIRECT

Virology 330 (2004) 105–115

VIROLOGY

www.elsevier.com/locate/yviro

A conserved secondary structure in the hypervariable region at the 5′ end of *Bamboo mosaic virus* satellite RNA is functionally interchangeable

Wen-Bin Yeh[a], Yau-Heiu Hsu[b], Hsin-Chuan Chen[c], Na-Sheng Lin[c,*]

[a]*Department of Biology, Kaoshiung Medical University, Kaoshiung, Taiwan 807, Republic of China*
[b]*Graduate Institute of Biotechnology, National Chung Hsing University, Taichung, Taiwan 402, Republic of China*
[c]*Institute of Botany, Academia Sinica, Nankang, Taipei, Taiwan 115, Republic of China*

Received 3 June 2004; returned to author for revision 2 July 2004; accepted 14 September 2004
Available online 13 October 2004

Abstract

Satellite RNA (satRNA) associated with *Bamboo mosaic virus* (BaMV) is dependent on BaMV for replication and encapsidation. Molecular analyses of total RNA extracted from bamboo species collected worldwide revealed that 26 out of 61 BaMV isolates harbored satBaMV. Among them, two phylogenetically distinguishable groups, A and B, with a genetic diversity of 6.9 ± 0.7% were identified. Greatest sequence diversity occurred in the 5′ untranslated region (UTR) that contained one hypervariable region with variations of up to 20.7%. Concurrent covariations in the 5′ hypervariable sequences support the existence of a conserved apical hairpin stem-loop structure, which was earlier mapped by enzymatic probings and functional analyses [Annamalai, P., Hsu, Y.H., Liu, Y.P., Tsai, C.H., Lin, N.S., 2003. Structural and mutational analyses of *cis*-acting sequences in the 5′-untranslated region of satellite RNA of bamboo mosaic potexvirus. Virology 311 (1), 229–239]. Furthermore, chimeric satBaMVs generated by interchanging the hypervariable region between groups A and B demonstrated the replication competence of satBaMV isolates in *Nicotiana benthamiana* protoplasts co-inoculated with BaMV RNA. The results suggest that an evolutionarily conserved secondary structure exists in the hypervariable region of 5′ UTR of satBaMV.

Keywords: Hypervariable region; *Bamboo mosaic virus*; Satellite RNA

Introduction

Populations of RNA viruses contain great genetic heterogeneity as a result of error-prone replication of RNA genomes (Domingo and Holland, 1994). The quasispecies nature of RNA viruses provides an effective way to explore new genomic sequences, which may adapt or evolve through a selection process (Domingo and Holland, 1994; Eigen et al., 1988). Thus, populations of RNA viruses with diversified biological properties appear to be relatively genetically stable (Garcia-Arenal et al., 2001). The apparent phylogenetic diversities within these populations have been analyzed according to nucleotide sequences for a number of plant RNA viruses (Garcia-Arenal et al., 2001). Such analyses have also been conducted for some subviral RNAs including the satellite RNAs of *Cucumber mosaic virus* (CMV) (Garcia-Arenal and Palukaitis, 1999; Grieco et al., 1997), *Rice yellow mottle virus* (RYMV) (Pinel et al., 2003) and *Turnip crinkle virus* (TCV) (Simon, 1999), satellite *Tobacco mosaic virus* (STMV) (Dodds, 1999), *Potato spindle tuber viroid* (Gast et al., 1996), *Grapevine yellow speckle viroid* (Polivka et al., 1996), and *Peach latent mosaic viroid* (Ambros et al., 1998; Pelchat et al., 2000). Among these subviral RNAs, several secondary structures have been proposed based on chemical and enzymatic probing studies. The secondary structures appear to be maintained despite some divergences in the primary sequence (Ambros et al., 1998; Fraile and Garcia-Arenal, 1991; Garcia-Arenal and Palukaitis, 1999; Gast et al., 1996; Pelchat et al., 2000; Simon, 1999).

Bamboo mosaic virus (BaMV), a potexvirus member of the alphavirus-like superfamily, infects at least 13 economically important bamboo species in Taiwan (Lin et al., 1993)

* Corresponding author. Fax: +886 2 27880991.
E-mail address: nslin@sinica.edu.tw (N.-S. Lin).

0042-6822/$ - see front matter © 2004 Elsevier Inc. All rights reserved.
doi:10.1016/j.virol.2004.09.025

and is mechanically transmissible through vegetative propagation. More than 80% of the two major cultivars, namely, Ma bamboo (*Dendrocalammus latiflorus* Munro) and Green bamboo (*Bambusa oldhamii* Munro), are infected (Lin et al., 1993).

BaMV contains a 6.4-kb single-stranded, positive-sense RNA genome with five conserved open reading frames (ORFs) (Lin et al., 1994; Yang et al., 1997). ORF1 encodes a protein of 155 kDa with three functional domains: an N-terminal methyltransferase, a central RNA helicase, and a C-terminal RNA-dependent RNA polymerase (RdRp) (Li et al., 1998, 2001). A triple gene block consisting ORFs 2–4 encode proteins of 28, 13, and 6 kDa, respectively. These triple gene block proteins are required for virus cell-to-cell movement (Chang et al., 1997; Lin et al., 2004; Wung et al., 1999). The product of ORF 5 is the capsid protein (CP) of 25 kDa.

BaMV RNA is 5′ capped and 3′ polyadenylated. The 3′ untranslated region (UTR) contains four major stem loops (domains A, B, C, and D) and a functional pseudoknot domain comprising at least 13 adenylate residues of the 3′ poly (A) tail (Cheng and Tsai, 1999; Tsai et al., 1999a). Domain D and pseudoknot are recognized by RdRp and are important for the initiation of minus strand RNA synthesis (Huang et al., 2001). The highly conserved potexviral hexanucleotides (ACc/uUAA) are located in the loop D (Cheng and Tsai, 1999).

Satellite RNA of BaMV (satBaMV) represents the lone example of satellite RNA found among the potexvirus group. This RNA molecule is fully dependent on BaMV for replication and encapsidation (Lin and Hsu, 1994). It contains an ORF for a 20-kDa protein (P20) flanked by a 5′ UTR of 159 nucleotides (nts) and a 3′ UTR of 125 nts. Structural and functional analyses of the 5′ UTR of BSF4 satBaMV revealed a long stem loop (LSL) and a small stem loop. The former comprises one apical loop, five internal loops, and a four-way junction short stem-loop, which are required for the efficient replication of satBaMV in BaMV co-infected cells (Annamalai et al., 2003). However, P20 is not essential for satBaMV replication (Lin et al., 1996) and shares 46% amino acid identity with CP of satellite virus associated with *Panicum mosaic virus* (Liu and Lin, 1995).

Previously, we have shown that seven isolates of satBaMV from different bamboo species and different localities displayed a nucleotide divergence from 0.7% to 7.5% (Liu et al., 1997). However, transcripts from infectious cDNA clones of satBaMV, pBSF4, and pBSL6 showed a differentially adaptive effect during co-inoculation with BaMV RNA (Hsu et al., 1998). Prototype BSF4 satBaMV did not significantly interfere with the BaMV replication, whereas transcripts from pBSL6 markedly reduced the symptom expression and accumulation of BaMV RNA in co-infected *Nicotiana benthamiana* plants (Hsu et al., 1998).

In the present study, we have characterized the genetic diversity among the satBaMV isolates from bamboo imported worldwide as well as from local varieties of Taiwan. Based on the phylogenetic analysis, two separate satBaMV lineages were identified. The greatest diversity is found in the 5′ UTR containing a hypervariable region. In spite of the vast sequence diversity in this region, the secondary structure of RNA displayed a conserved topology. Furthermore, the hypervariable sequence was interchangeable between the two isolates belonging to two lineages. The results indicate that the RNA secondary structure in the hypervariable region of 5′ UTR of satBaMV is evolutionarily conserved.

Results

Detection and phylogeny of satBaMV isolates

Infection of BaMV and satBaMV in the collected bamboo leaves showing mosaic symptoms was confirmed by RNA dot blot hybridization (Table 1). Except in isolate BB18, BaMV RNA was detected in 60 out of 61 bamboo samples. However, BaMV genomic RNA could be demonstrated by reverse transcription-polymerase chain reactions (RT-PCR) in BB18 (data not shown). The inability of detection of BaMV RNA in BB18 was probably due to low accumulation. Out of 61 samples, 26 were positive for satBaMV (Table 1). Among the 26 samples, 17 isolates were from all the BaMV-infected Ma bamboo (*D. latiflorus*), whereas only 2 from the 23 BaMV infected Green bamboo (*B. oldhamii*) were positive for satBaMV. The remaining seven positive satBaMV detections were in *B. vulgaris* (BV17 and BB25), *D. giganteus* (BB18), *Gigantochloa levis* (BB21), *B. pachinensis* (BB23 and BB26), and *B. edulis* (BB28) (Table 1). Chi-square analysis significantly showed host-based prevalence ($\chi^2 = 29.1$, $df = 1$, $P < 0.001$) between Ma and Green bamboo.

From each infected plant, virions were purified and viral RNA was extracted. Subsequently, full-length cDNA of satBaMV was amplified by RT-PCR and sequenced. Phylogenetic analyses were performed using the Neighbor-Joining clustering and Maximum Parsimony methods. As shown in Fig. 1, separate and pronounced evolving processes occur in two lineages as the branch lengthened between the nodes, A (n_A) and B (n_B). Based on this result, the isolates were categorized into two major groups, A and B. Isolates belonging to group A were mostly derived from the *Bambusa* species, including *B. edulis*, *B. oldhamii*, *B. pachinensis*, *B. vulgaris*, etc., as well as from a few species of *Dendrocalamus*. Isolates of group B were all from *D. latiflorus* except BB21, which was from *G. levis.* It is also evident that none of the isolates showed significant correlation to the geographical distribution. For example, isolates DL15 and DL16 though collected from the neighborhood area did not fall in the same cluster (Fig. 1). In contrast, isolates BSL3 and BSL6 collected from two distinct areas could be grouped together (Fig. 1 and Liu et al., 1997).

Table 1
Detection of BaMV and satBaMV RNAs from different bamboo species and localities by dot blot hybridization

satBaMV isolates[a]	Accession no.	Host species[b]	Longitude	Latitude	Date	BaMV[c]	SatBaMV[d]
DL6V1	AY205200	*D. latiflorus*	1213037E	250152N	07/06/1997	+	+
DL6V6	AY205206	*D. latiflorus*	1213037E	250152N	07/06/1997	+	+
DLI-1	AY205159	*D. latiflorus*	1213037E	250152N	08/15/1998	+	+
DLII-1	AY205169	*D. latiflorus*	1213037E	250152N	08/15/1998	+	+
DLIII-1	AY205178	*D. latiflorus*	1213037E	250152N	08/15/1998	+	+
DLIV-1	AY205187	*D. latiflorus*	1213037E	250152N	08/15/1998	+	+
DL11	AY205211	*D. latiflorus*	1203621E	222541N	02/16/1999	+	+
DL12	AY205212	*D. latiflorus*	1204256E	242807N	02/18/1999	+	+
DL15	AY205213	*D. latiflorus*	1204250E	240646N	05/16/1999	+	+
DL16	AY205214	*D. latiflorus*	1204018E	235426N	06/12/1999	+	+
DL17	AY205223	*D. latiflorus*	1203248E	233846N	06/12/1999	+	+
DL18		*D. latiflorus*	1202247E	233400N	06/12/1999	+	+
DL19	AY205224	*D. latiflorus*	1203430E	230403N	06/20/1999	+	+
DL20	AY205225	*D. latiflorus*	1203736E	225413N	06/20/1999	+	+
DL21	AY205226	*D. latiflorus*	1214347E	244450N	10/25/1999	+	+
DL22		*D. latiflorus*	1213250E	235656N	10/26/1999	+	+
DL23	AY205215	*D. latiflorus*	1212350E	233706N	10/26/1999	+	+
BV11		*B. vulgaris*	1202107E	235832N	02/17/1999	+	–
BV13		*B. dolichoclada*	1213037E	250152N	02/23/1999	+	–
BV17	AY205222	*B. vulgaris*	1213037E	250152N	01/19/1999	+	+
BO11		*B. oldhamii*	1202952E	225321N	02/15/1999	+	–
BO12		*B. oldhamii*	1204256E	242807N	02/18/1999	+	–
BO13		*B. oldhamii*	1204217E	235600N	02/21/1999	+	–
BO14		*B. oldhamii*	1203619E	240452N	02/21/1999	+	–
BO16		*B. oldhamii*	1201923E	225815N	03/29/1999	+	–
BO17		*B. oldhamii*	1201851E	225901N	03/29/1999	+	–
BO18		*B. oldhamii*	1201103E	230924N	03/29/1999	+	–
BO19		*B. oldhamii*	1205705E	243733N	04/03/1999	+	–
BO20	AY205220	*B. oldhamii*	1213626E	250143N	04/20/1999	+	+
BO22		*B. oldhamii*	1204250E	240646N	05/16/1999	+	–
BO23	AY205221	*B. oldhamii*	1211041E	244747N	05/16/1999	+	+
BO24		*B. oldhamii*	1211607E	245320N	05/16/1999	+	–
BO25		*B. oldhamii*	1204637E	235013N	06/12/1999	+	–
BO26		*B. oldhamii*	1203736E	225413N	06/20/1999	+	–
BO27		*B. oldhamii*	1203430E	230403N	06/20/1999	+	–
BO28		*B. oldhamii*	1202704E	232917N	06/20/1999	+	–
BO29		*B. oldhamii*	1212146E	245447N	07/26/1999	+	–
BO30		*B. oldhamii*	1212750E	245757N	07/26/1999	+	–
BO31		*B. oldhamii*	1213107E	245837N	07/26/1999	+	–
BO32		*B. oldhamii*	1214812E	243724N	10/25/1999	+	–
BO33		*B. oldhamii*	1213250E	235656N	10/26/1999	+	–
BO34		*B. oldhamii*	1213711E	250231N	07/30/2000	+	–
BB1		*B. utilis*	1204004E	225826N	01/17/1999	+	–
BB2		*B. pachinensis*	1204004E	225826N	01/17/1999	+	–
BB3		*B. oldhamii*	1204004E	225826N	01/17/1999	+	–
BB4		*D. strictus*	1204004E	225826N	01/17/1999	+	–
BB5		*D. giganteus*	1204004E	225826N	01/17/1999	+	–
BB12		*B. vulgaris*	1213037E	250152N	02/23/1999	+	–
BB13		*B. ventricosa*	1213037E	250152N	02/23/1999	+	–
BB14		*B. dolichoclada*	1213037E	250152N	02/23/1999	+	–
BB18	AY205216	*D. giganteus*	1213037E	250152N	08/19/1999	–[e]	+
BB19		*B. tulda*	1213037E	250152N	05/18/1999	+	–
BB20		*B. dolichomerithalla*	1213037E	250152N	05/18/1999	+	–
BB21	AY205199	*G. levis*	1213037E	250152N	05/18/1999	+	+
BB22		*B. edulis*	1202704E	232917N	06/20/1999	+	–
BB23	AY205217	*B. pachinensis*	1213037E	250152N	08/19/1999	+	+
BB24		*B. dolichoclada*	1213037E	250152N	08/19/1999	+	–
BB25	AY205218	*B. vulgaris*	1141417E	222340N	08/19/1999	+	+
BB26		*B. pachinensis*	1214246E	244633N	10/25/1999	+	+
BB27		*P. japonica*	1214246E	244633N	10/25/1999	+	–
BB28	AY205219	*B. edulis*	1210532E	225013N	10/26/1999	+	+

(continued on next page)

Table 1 (*continued*)

satBaMV isolates[a]	Accession no.	Host species[b]	Longitude	Latitude	Date	BaMV[c]	SatBaMV[d]
BSF4	L22762	*B. vulgaris*	1213037E	250152N	Liu et al., 1997[f]	+	+
BSL1	L78260	*D. latiflorus*	1202704E	232917N	Liu et al., 1997[f]	+	+
BSL2	L78261	*B. beecheyana*	1204004E	225826N	Liu et al., 1997[f]	+	+
BSL3	L78262	*B. dolichoclada cv.*	1202704E	232917N	Liu et al., 1997[f]	+	+
BSL4	L78263	*P. usawai*	1202704E	232917N	Liu et al., 1997[f]	−[e]	+
BSL6	L78264	*D. latiflorus*	1213037E	250152N	Liu et al., 1997[f]	+	+
USA1	L78265	*B. beecheyna*	1170904W	324412N	Liu et al., 1997[f]	+	+

[a] Abbreviations of satBaMV isolates: capital letters are bamboo species and the numbers are the collecting order.
[b] *D*: *Dendrocalamus*; Ma Bamboo (*D. latiflorus*) *B*: *Bambusa*; Green Bamboo (*B. oldhamii*) *G*: *Gigantochloa*; *P*: *Pseudosasa*.
[c] +, BaMV RNA positively detected.
[d] +, satBaMV RNA positively detected; −, no satBaMV RNA detected.
[e] −: dot blot negative, but RT-PCR positive.
[f] References of the reported isolates.

Sequence of the full-length cDNA clones of satBaMV was aligned using the Pileup program from the GCG package. Genetic diversity calculations from proportion models revealed two distinct groups among these isolates, a result that is consistent with the phylogenetic analyses. Divergence between the two groups ranged from 0.054 to 0.084 with an average of 0.069 (Table 2), while the sequence divergence within each group ranged from 0.002 to 0.048.

Sequence variation in the 5′ UTR, P20 coding region, and 3′ UTR

Analysis of nucleotide sequence revealed that 30 satBaMV isolates, including the previously collected isolates (Liu et al., 1997), were similar in length (830–837 nts). Of the total 836 nts of prototype BSF4 satBaMV, 159, 552, and 125 nts constituted the 5′ UTR, P20 coding region, and 3′ UTR, respectively (Lin and Hsu, 1994). The 5′ UTR sequences displayed the greatest genetic variation of 0.090 ± 0.019 between groups A and B (Table 2). This includes a significant variation of up to 0.207 between nt 54 and 92, which is identified as the hypervariable region. The sequences of 5′ UTR of 30 isolates from 14 localities are shown in Fig. 2.

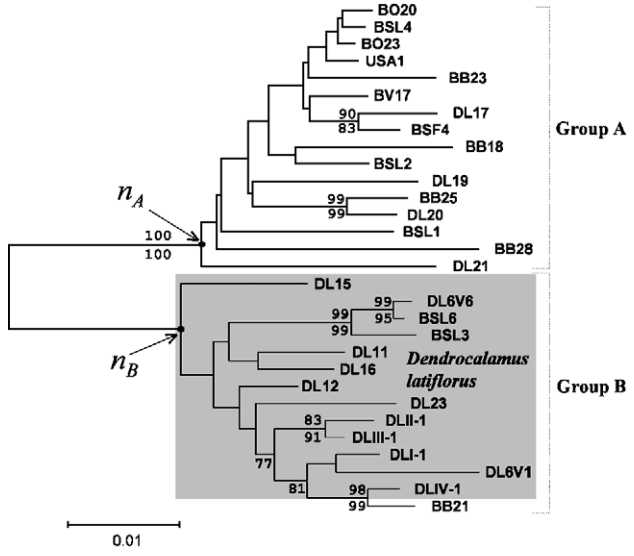

Fig. 1. Phylogram of full-length satBaMV isolates constructed using the Neighbor-Joining clustering method. The branch length is proportional to the divergence scale (0.01). Bootstrap values greater than 70 are shown above the branch. Analysis from Maximum Parsimony method obtained a similar tree topology and the bootstrap values were shown beneath the branch. Isolates in group B from Ma bamboo (*D. latiflorus*) are shadowed.

The ORF of P20 is present in every isolate sequenced to date and both the termini of P20 are relatively conserved. Nucleotide variations for P20 coding region within groups A and B, and between the two groups are 0.024 ± 0.003 and 0.070 ± 0.010, respectively, with values similar to those of full-length satBaMV (Table 2). Amino acid variation of P20 was 0.053 ± 0.013 between the two groups. The divergence of P20 codon positions when analyzed revealed that the variation for the third position of P20 codons was about four times higher than that for the first or second positions. The d_{NS}/d_S ratio (nonsynonymous substitution/synonymous substitution) for P20 in both groups A and B is 0.14.

Sequence of the 3′ UTR showed the least diversity (0.036 ± 0.011) of the whole satBaMV molecule (Table 2). This trend is also reflected in other subviral RNAs (Danthinne et al., 1991; Dodds, 1999; Kurath et al., 1993). Conserved hexanucleotides (ACCTAA), which are common in potexviruses and carlaviruses (White et al., 1992), and the polyadenylation signal (AATAAA) are present in all the satBaMV isolates.

Distinct evolutionary patterns occur in the 5′ UTR and P20 coding region

To reveal the genetic diversity of satBaMVs, separate calculations were performed for substitution transition (Ts; purine–purine or pyrimidine–pyrimidine exchange) and transversion (Tv; purine–pyrimidine or pyrimidine–purine exchange). The relative coefficients in transversion (R_{Tv}) or transition (R_{Ts}) vs. total substitutions in the P20 coding region are shown in Fig. 3B. These substitutions revealed extremely different evolving processes for the 5′ UTR and P20 coding regions. The evolved process of transversion is

Table 2
Substitution divergence among satBaMV isolates

Isolates	5′ UTR	P20 coding region		3′ UTR	Full length
		nt	aa		
Within group A	0.044 ± 0.009	0.024 ± 0.003	0.014 ± 0.004	0.022 ± 0.008	0.027 ± 0.003
Within group B	0.039 ± 0.009	0.024 ± 0.003	0.014 ± 0.004	0.022 ± 0.009	0.026 ± 0.003
Between groups A and B	0.090 ± 0.019	0.070 ± 0.010	0.053 ± 0.013	0.036 ± 0.011	0.069 ± 0.007
	1st	2nd	3rd		
Within group A	0.008 ± 0.003	0.007 ± 0.002	0.057 ± 0.007		
Within group B	0.008 ± 0.003	0.009 ± 0.003	0.055 ± 0.009		
Between groups A and B	0.032 ± 0.012	0.032 ± 0.012	0.147 ± 0.019		

UTR: untranslated region; nt: nucleotide; aa: amino acid; 1st, 2nd, and 3rd: the first, second, and third position of P20 codon, respectively.

similar to that of the transition in the 5′ UTR (Fig. 3A). However, in the P20 coding region, transversion was less significant than transition that was about fivefold higher (Fig. 3B). Substitution pattern in the 3′ UTR was not calculated due to the insignificant sequence variation.

The hypervariable region folds into a conserved secondary structure in the 5′ UTR

Sequence analyses of satBaMV isolates revealed a hypervariable region at nt 54–92 in the 5′ UTR (Fig. 2). The proposed folding for the 5′ hypervariable region of the prototype BSF4 satBaMV comprises an apical loop followed by two internal-loops interwoven by 3–4, 2, and 5 base-paired stems (Annamalai et al., 2003) (Fig. 4), which is designated as the apical hairpin stem-loop (AHSL). To depict the significance of AHSL, RNA secondary structure of the hypervariable region of 30 satBaMV isolates was predicted by the MFOLD software. Results from the prediction indicated that most of the isolates (22 out of 30) retained a nearly identical AHSL structure regardless of whether the isolates are from group A or B (Fig. 4, boxed). Although the folding of other eight isolates is not well conserved, they exhibit a similar hairpin stem-loop structure. The predicted AHSL structure of hypervariable region showed compensatory changes primarily in the base-paired stem regions while most variable sites appeared in the loop.

To further determine whether these changes in the stem regions occurred at random, we tallied all the observed single and double compensatory stem substitutions. Substitutions in the stem region were analyzed if such changes will disrupt or maintain the base pairing. For RNA molecules, the probability of a double substitution converting one pair of complementary base to another pair is 0.256, and the value for single substitution is 0.125 (Dixon and Hillis, 1993). From the two prototypes, BSF4 (group A) and BSL6 (group B), a total of 31 substitutions comprising 22 isolates (boxed in Fig. 4) were constructed in the stem region. As shown in Fig. 4, most of the substitutions did not disrupt the pairings in the stem regions. Twenty-nine compensatory changes were observed, including 15 single base pairing to base pairing and 7 double base pairing to base pairing. Based on these data, 5.7 changes are expected by random mutation, including 2.1 single base pairing to base pairing and 1.8 double base pairing to base pairing (Table 3). However, the observed compensatory mutations are significantly higher than the expected ones (χ^2 = 90.4

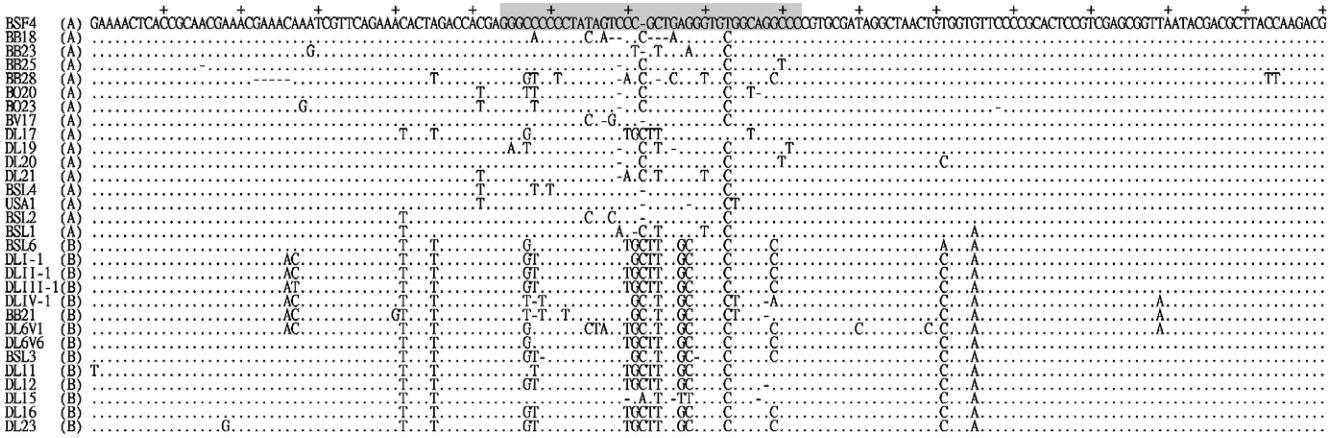

Fig. 2. Nucleotide sequences of the 5′ UTR of satBaMV isolates. Nucleotides identical to those of the BSF4 isolate are indicated by a dot (.), and gaps are indicated by a dash (−). Hypervariable sequences (nt 54–92) for the simulation of RNA secondary structure are boxed.

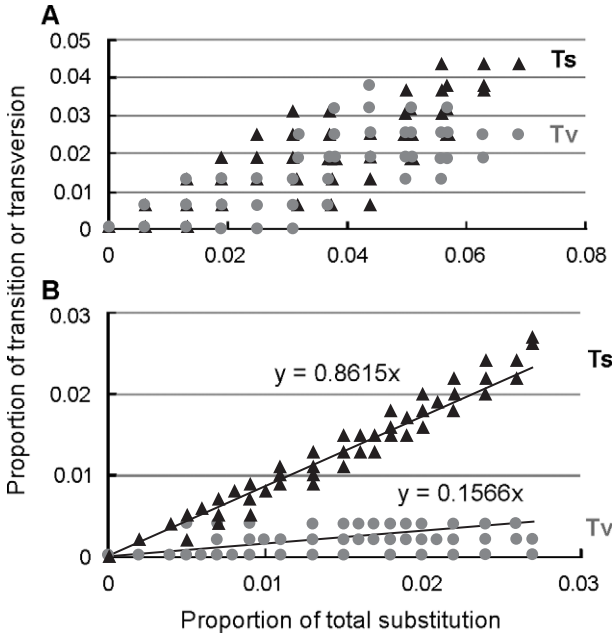

Fig. 3. Scatter plots of transition (Ts, triangle) or transversion (Tv, circle) of the 5′ UTR (A) and the P20 coding region (B) versus total substitution (Tvs) for all pairwise comparisons. Relative coefficients are shown in the panel.

and $\chi^2 = 32.2$, $df = 1$, $P < 0.001$, for single and double substitutions, respectively). Even for the remaining eight isolates (out of the box in Fig. 4), similar significant results were obtained ($\chi^2 = 62.5$ and $\chi^2 = 11.6$, $df = 1$, $P < 0.001$, for single and double substitutions, respectively) (data not shown). These results suggest that the secondary AHSL structure exists within the hypervariable region of 5′ UTR of satBaMV isolates.

Chimeric satBaMVs with interchanged AHSL are replication competent

Earlier enzymatic probings and mutational analyses showed that the 5′ UTR of BSF4 satBaMV folds into a LSL and a small stem loop (Annamalai et al., 2003). By MFOLD prediction, the 5′ UTR of BSL6 folds into five stem-loop structures (Fig. 5A). Subsequently, in order to determine whether the conserved secondary structure in the hypervariable region is involved in satBaMV replication, the hypervariable sequences of pBSF4 from group A and pBSL6 from group B were interchanged. The resulted full-length satBaMV clones, pBSF20 and pBSF21, retained their parental RNA secondary structure by MFOLD predictions (Fig. 5A).

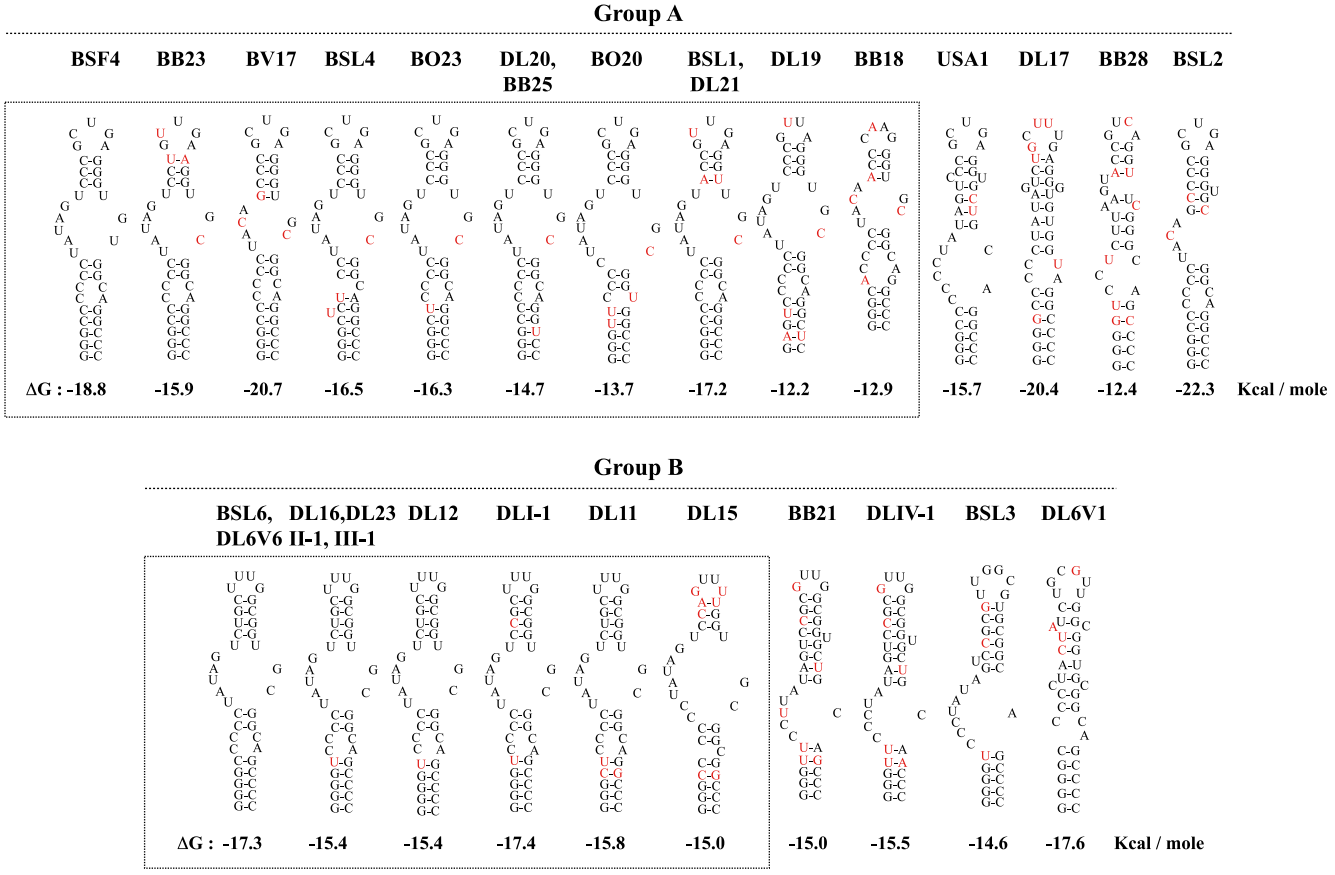

Fig. 4. Secondary structure of the hypervariable region of natural satBaMV isolates. The structures were simulated from nt 54 to 92 of satBaMV isolates from groups A and B by MFOLD Program version 3.1 (Zuker et al., 1999). Most of the isolates (22 out of 30) have a nearly identical prediction (within the box). The variable sites corresponding to BSF4 (group A) or BSL6 (group B) are shown in red.

Table 3
Substitutions in the hypervariable stem regions of satBaMV isolates based on the secondary structure shown in Fig. 4

Type of substitution	No. expected[a]	No. observed	*P*
Single			<0.001
Base pairing to base pairing	2.1	15	
Base pairing to non-base pairing	14.9	2	
Double			<0.001
Base pairing to base pairing	1.8	7	
Base pairing to non-base pairing	5.2	0	

[a] The no. expected in single base pairing to base pairing is (15 + 2) × 0.125 = 2.1, and the value for single base pairing to non-base pairing is (15 + 2) − 2.1 = 14.9.

The replication ability of the chimeric BSF20 and BSF21 was tested in protoplasts of *N. benthamiana* co-inoculated with BaMV RNA. Twenty-four hours after inoculation, protoplasts were harvested for Northern blot analysis by satBaMV-specific probe. The accumulation levels of BSF20 and BSF21 were similar to those of BSF4 and BSL6 satBaMVs in co-inoculated protoplasts with BaMV RNA (Fig. 5B). In control experiments, satBaMV was not detected in protoplasts inoculated with any satBaMV alone (data not shown), indicating that the signals in Fig. 5B are not due to contamination of the input RNAs. The results suggest that BSF20 and BSF21 are replication competent.

Discussion

Detection and phylogeny of satBaMV isolates

Although the origin of satellite RNA has been intrigued, information on the natural prevalence of satellite RNA is quite limited (Roossinck et al., 1992; Simon et al., 2004; Vogt and Jackson, 1999). The prevalence of satellite RNA varies and for instance, high (75%) in RYMV satRNA (Pinel et al., 2003) but low (30%) in CMV satRNA even though CMV satRNA occurs all over the world (Garcia-Arenal et al., 2000). In both cases, the prevalence of satellite RNA is variable among regions. According to our investigation, the frequency of satBaMV in the field populations of BaMV seems to be less than 50%. From the phylogenetic analysis, the prevalence of two evolutionary lineages, A and B, has no correlation with geographic locations. Interestingly, satBaMVs showed host preference for the two most common bamboo hosts, Ma bamboo and Green bamboo (Fig. 1). All the collected BaMV isolates originated from Ma bamboo (*D. latiflorus*) harbored group-B-like satBaMV RNAs whereas only 9% Green bamboo BaMV isolates associated group-A-like satBaMVs (Table 1) in spite of more than 80% of BaMV incidence in Green bamboo plantation in Taiwan (Lin et al., 1993). Isolates of BSF4 and BSL6, originally from *B. vulgaris* (Lin and Hsu, 1994) and *D. latiflorus* (Liu et al., 1997), respectively, replicated efficiently in protoplasts of Green bamboo in the presence of BaMV RNA (Lin, N.S., unpublished results), indicating that factors other than replication such as cell-to-cell movement, long-distance movement, etc., determine the specific interaction with host. Hence, in accordance with earlier report (Simon et al., 2004), it is evident that the species of host play an important role in the selection of satBaMV RNA populations.

Hypervariation in the 5′ UTR of satBaMV

SatBaMV belongs to the messenger-type satRNAs and the information on genetic variations of messenger type

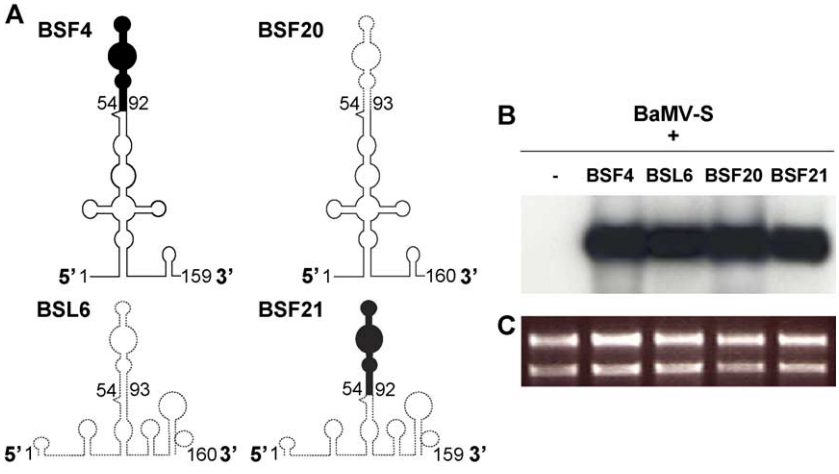

Fig. 5. Schematic RNA secondary structure of 5′ UTRs and inoculation assay of chimeric satBaMVs. (A) RNA secondary structures in the 5′ UTRs predicted by the MFOLD program version 3.1 (Zuker et al., 1999). Nucleotides in the 5′ UTR are from 1 to 159 and nucleotides in the hypervariable sequence are from 54 to 92. Sequences derived from BSF4 satBaMV represented as solid lines (hypervariable region in dark background) while sequences from BSL6 as dotted lines. (B) Accumulation of satBaMV RNAs in protoplasts of *N. benthamiana* co-inoculated with BaMV RNA. RNA samples were extracted from 3 × 10^4 protoplasts, 24 h after inoculation, and analyzed by Northern blot with satBaMV-specific probe (Lin et al., 1996). RNA transcripts of BaMV and satBaMV isolates or mutants were indicated above each lane. Lane −: no satBaMV RNA added. (C) Ethidium bromide staining of the gel prior to blotting shows equal loading as revealed by ribosomal RNA abundance in each lane.

satRNA is limited. SatBaMV isolates between group A and B displayed sequence diversity of 6.9%, which is consistent with variations reported for plant virus satRNAs (Garcia-Arenal et al., 2001). The 5′ UTR containing the hypervariable region showed the most divergence of the whole molecule (Fig. 2 and Table 2). Hypervariable regions have been reported in subviral RNA (Palukaitis and Roossinck, 1995) as well as RNA virus genomes, including noncoding and coding region (Kurosaki et al., 1995; Shurtleff et al., 2001; Sumi et al., 1999). These hypervariable regions are highly divergent as a result of substitution, deletion, or insertion during replication cycle, which might play a role in the evolution or the virulence of RNA molecules (Leitmeyer et al., 1999; Shurtleff et al., 2001). In the case of CMV satRNA, the hypervariability is suggested to be affected by the quasispecies nature of the helper viruses and the sequence content of satRNA (Palukaitis and Roossinck, 1995). However, the sequence of the satBaMV helper virus has not been determined yet.

Different selection pressure exists in the 5′ UTR and P20 coding region

It is generally accepted that transversion is limited to short-term evolution. For example, serial passages of CMV, TMV, and *Wheat streak mosaic virus* in experimental plants reveal only transition mutations (Hall et al., 2001; Roossinck, 2002; Schneider and Roossinck, 2000). In the present study, relative substitution of transversions vis-a-vis transitions revealed that transition bias occurred in the P20 coding region among the natural satBaMV isolates (Fig. 3B). However, a trend of equal number of transition and transversion showed a different evolution pattern in the 5′ UTR (Fig. 3A). Further examination of the *P20* gene using a neutral selection model indicated that the functional constraint of the coding region with a value of d_{NS}/d_S (0.140 and 0.141 of groups A and B, respectively) is similar to that of the coat proteins of other plant viruses (Garcia-Arenal et al., 2001). This functional constraint of the *P20* gene is further supported by the fact that P20 is involved in the satBaMV RNA binding and movement (Lin et al., 1996; Tsai et al., 1999a). Taken together, these findings suggest that the selective pressure in P20 coding region is at the protein level, while the selective pressure in the 5′ UTR is at RNA level.

RNA secondary structure of the hypervariable sequence as an evolutionary constraint

Previously enzymatic, mutational, and covariation analyses of the 5′ UTR of BSF4 satBaMV demonstrated a LSL structure that is required in *cis* for replication of satBaMV (Annamalai et al., 2003). The major stem structures in the LSL have a vital impact on satBaMV accumulation. Deletions or substitutions that disrupt stem formation substantially reduced the accumulation of satBaMV. Subsequently, in this study, a hypervariable region with a conserved AHSL secondary structure was identified in the 5′ UTR of natural isolates of satBaMV by MFOLD program and covariation analysis (Fig. 4). Although covariation analysis strengthens the AHSL structure, the potential long-distance base pairing, pseudoknot formation, and possible RNA–protein interactions cannot be predicted.

In the basal five base-paired stems of AHSL structure in BSF4 satBaMV, mutations that disrupted C/G and G/C base pairs resulted in the loss of replication ability (Annamalai et al., 2003). However, compensatory changes [either C/G (57/89) → U/A or G/C (55/91) → A/U, or alteration in five nucleotides] restored the activity of satBaMV mutants nearly to the wild-type level. It is evident that hypervariation results from the selection for compensatory mutations that maintain the secondary structure (Table 3). Maintenance of conserved RNA secondary structure that is constrained in the satBaMV evolution is further strengthened by the fact that the hypervariable AHSL regions between groups A and B are interchangeable in spite of their vast sequence divergence. This is evidenced by the replication competence of chimeric satBaMVs in infected protoplasts (Fig. 5). Furthermore, this AHSL region contains P20 core binding site with G- and U-rich sequences, ^{72}GCUGAGGGUGUGGCAGG0^{88}, which is involved in the formation of P20-RNA complexes (Tsai et al., 1999b). Thus, the conserved AHSL structure may be a bifunctional motif in the 5′ UTR, which modulates the replication and translation of satBaMV RNA.

Conserved secondary structures are of functional significance in viral replication, transcription, recombination, and pathogenesis by their highly conserved sequence or through the interaction of secondary structure with viral or cellular proteins (Garcia-Arenal et al., 2001; Hofacker et al., 2004; Roossinck et al., 1992). Thus, they are very sensitive to mutations in which few critical substitutions or about 10% mutation could result in the disruption of secondary structures, and consequently, loss of activity (Schuster et al., 1994). In this study, we present an evolutionarily conserved AHSL secondary structure in the satBaMV genome, most importantly within the hypervariable region. Hypervariation in naturally occurring sequence could lead to a wide range of satellite RNA population. Under selection pressure, there might be a strong constraint on the hypervariation to conserve potential RNA folding and function. Such hypervariability and potential RNA folding might be important features that mediate the interactions among satBaMV, helper virus, and host plants (Palukaitis and Roossinck, 1995). Although the importance of this motif in the interaction with helper virus and host plants needs further investigation, it should be noted that the AHSL structure has significant consequences in the evolution and biology of satBaMV RNA.

Materials and methods

Sample collection, detection of BaMV and satBaMV, and virus purification

Bamboo leaves with mosaic symptoms were collected from cultivated bamboos and bamboo nurseries in Taiwan, where different imported bamboo species from worldwide are grown. Table 1 lists the sampling numbers, longitude, latitude, and host species of satBaMV isolates. Seven previously reported isolates of BSF4, BSL1, BSL2, BSL3, BSL4, BSL6, and USA1 (Liu et al., 1997) were also included.

Total RNA was extracted from bamboo leaves and probed for BaMV and satBaMV RNA by dot blot hybridization (Lin et al., 1993, 1996). The in vitro ^{32}P-labeled RNA transcripts synthesized from pBaHB and pBSHE were the specific probes for the detection of BaMV and satBaMV RNA, respectively (Lin et al., 1993). For mini-purification of BaMV virions, 5 g of bamboo leaves was collected from each individual bamboo bush. BaMV virions were purified and the viral RNA was extracted as described previously (Lin and Chen, 1991). Chi-square analysis was used to test the parasitized association between satBaMV and its bamboo hosts (SAS Institute, 2001).

Construction and sequence determination of full-length cDNA of satBaMV RNA

Purified viral RNA was used as the template for RT-PCR to amplify the full-length cDNA of satBaMV RNA. Full-length cDNA of the satBaMV was synthesized by PCR with the following primers: BS19, 5′-TGCCTGCAG*TAATACGACTCACTATA*GAAAACTCACCGCAACGA-3 (*Pst*I site is underlined; T7 promoter sequence in italics; and the 5′ terminal 18 nts of satBaMV (Lin and Hsu, 1994) and polyadenylation primer BS43, 5′-GTCGACTCTAGAT$_{20}$-3′ (the *Xba*I site is underlined). Amplified cDNA fragment was then separated and isolated from 1% agarose, ligated into pGEM-T easy vector (Promega, Madison, WI) and transformed to *E. coli* DH5α. The resulting plasmids were selected and sequenced. Sequence was analyzed by ABI 377A Sequencer using the *Taq* dye Terminator Cycle Sequencing Kit (Applied Biosystems, Foster City, CA).

Sequence analysis

Multiple sequence alignment was done using the Pileup program of the GCG software package, which was then manually refined. The neutral selection model of Pamilo and Bianchi (1993) and Li (1993) was employed to fit the nonsynonymous (d_{NS}) and synonymous (d_S) substitution of isolates. Phylogenetic analyses were performed using Neighbor-Joining (NJ) and Maximum Parsimony (MP) methods provided by softwares MEGA version 2.1 and PHYLIP (Felsenstein, 1993; Kumar et al., 2001). Distance estimates of Kimura two-parameter model and the heuristic searching algorithm were used for NJ and MP analyses, respectively. Hairpin simulations for the hypervariable region in the 5′ UTR were analyzed using the MFOLD provided by the SeqWeb computer center (bioinfo.nhri.org.tw/), and hairpins with the least energy value were selected.

Construction of chimeric satBaMVs

Plasmids pBSF4 and pBSL6 are full-length cDNA clones of satBaMV with a T7 RNA promoter at the 5′ end (Hsu et al., 1998; Lin et al., 1996). To construct the chimeric satBaMVs, the hypervariable sequences of pBSF4 and pBSL6 were interchanged, and the mutants are designated as pBSF20 and pBSF21, respectively (Fig. 5A). The mutants were constructed by site-directed mutagenesis using a double-PCR method (Annamalai et al., 2003). For the construction of pBSF20, the first PCR product was synthesized from the pBSF4 template using primers BS19, and BSF20R (5′-CGGGGGCTGCCGCACCGCCAAAG-CAGACTATAGGGGGCCCCTCGTGGTCT-3′), followed by the second PCR using pBSF4 as template with primer BS43 and the first PCR product. The *Pst*I- and *Xba*I-digested secondary PCR fragments were ligated with the *Pst*I- and *Xba*I-cut pBSF4 to generate pBSF20. To generate pBSF21, the first PCR product was synthesized from pBSL6 template by primers BS19 and BSF21R (5′-GCACGGGGCCTGCCACACCCTCAGCGGGACTA-TAGGGGGGCCCTCGTG-3′), followed by the second PCR using pBSL6 as template with primer BS24 (5′-CCTTCTCGAGT$_{15}$-3′, *Xho*I site underlined) and the first PCR fragments. The *Pst*I- and *Xho*I-digested secondary PCR fragments were ligated to the *Pst*I- and *Xho*I-cut pBSL6.

In vitro transcription

Transcription utilized plasmids pCB, pBSF4, and pBSL6. pCB is an infectious clone of BaMV-S (Lin et al., 2004) while pBSF4 and pBSL6 are infectious clones of satBaMV (Hsu et al., 1998; Lin et al., 1996). Conditions for in vitro transcription were as previously described (Lin et al., 1996).

Protoplast inoculation, RNA extraction, and Northern blot analyses

Preparation and RNA inoculation of protoplasts from *N. benthamiana* were carried out as previously described (Lin et al., 1996). For each inoculation, protoplasts of 2×10^5 cells were inoculated with either 1.0 μg of BaMV-S RNA only or co-inoculated with 1.0 μg of various satBaMV transcripts by electroporation. Total RNA extraction, glyoxylation, and Northern blot analyses with ^{32}P-labeled satBaMV-specific probe were carried out as previously described (Lin et al., 1996).

Acknowledgments

We thank Drs. P.C. Huang, J.H. Shih and P.V. Palani for critical review of manuscript, and Miss M.Z. Fang for sequencing service. This research was supported in part by National Science Council Project Grant NSC89-2311-B-001-021, NSC89-2811-B-001-061 and NSC 90-2321-B-001-001 and by the Academia Sinica, Taipei, Taiwan.

References

Ambros, S., Hernandez, C., Desvignes, J.C., Flores, R., 1998. Genomic structure of three phenotypically different isolates of peach latent mosaic viroid: implications of the existence of constraints limiting the heterogeneity of viroid quasispecies. J. Virol. 72 (9), 7397–7406.

Annamalai, P., Hsu, Y.H., Liu, Y.P., Tsai, C.H., Lin, N.S., 2003. Structural and mutational analyses of *cis*-acting sequences in the 5′-untranslated region of satellite RNA of bamboo mosaic potexvirus. Virology 311 (1), 229–239.

Chang, B.Y., Lin, N.S., Liou, D.Y., Chen, J.P., Liou, G.G., Hsu, Y.H., 1997. Subcellular localization of the 28 kDa protein of the triple-gene-block of bamboo mosaic potexvirus. J. Gen. Virol. 78 (Pt. 5), 1175–1179.

Cheng, C.P., Tsai, C.H., 1999. Structural and functional analysis of the 3′ untranslated region of bamboo mosaic potexvirus genomic RNA. J. Mol. Biol. 288 (4), 555–565.

Danthinne, X., Seurinck, J., Van Montagu, M., Pleij, C.W., van Emmelo, J., 1991. Structural similarities between the RNAs of two satellites of tobacco necrosis virus. Virology 185 (2), 605–614.

Dixon, M.T., Hillis, D.M., 1993. Ribosomal RNA secondary structure: compensatory mutations and implications for phylogenetic analysis. Mol. Biol. Evol. 10 (1), 256–267.

Dodds, J.A., 1999. Satellite tobacco mosaic virus. Curr. Top. Microbiol. Immunol. 239, 145–157.

Domingo, E., Holland, J.J., 1994. Mutation rates and rapid evolution of RNA viruses. In: Morse, S.S. (Ed.), The Evolutionary Biology of Viruses. Raven Press, New York, pp. 161–184.

Eigen, M., McCaskill, J., Schuster, P., 1988. Molecular quasispecies. J. Phys. Chem. 92, 6881–6891.

Felsenstein, J., 1993. PHYLIP (Phylogeny Inference Package), version 3.5. Department of Genetics, University of Washington, Seattle, WA, USA.

Fraile, A., Garcia-Arenal, F., 1991. Secondary structure as a constraint on the evolution of a plant viral satellite RNA. J. Mol. Biol. 221, 1065–1069.

Garcia-Arenal, F., Escriu, F., Aranda, M.A., Alonso-Prados, J.L., Malpica, J.M., Fraile, A., 2000. Molecular epidemiology of Cucumber mosaic virus and its satellite RNA. Virus Res. 71 (1–2), 1–8.

Garcia-Arenal, F., Fraile, A., Malpica, J.M., 2001. Variability and genetic structure of plant virus populations. Annu. Rev. Phytopathol. 39, 157–186.

Garcia-Arenal, F., Palukaitis, P., 1999. Structure and functional relationships of satellite RNAs of cucumber mosaic virus. Curr. Top. Microbiol. Immunol. 239, 37–63.

Gast, F.U., Kempe, D., Spieker, R.L., Sanger, H.L., 1996. Secondary structure probing of potato spindle tuber viroid (PSTVd) and sequence comparison with other small pathogenic RNA replicons provides evidence for central non-canonical base-pairs, large A-rich loops, and a terminal branch. J. Mol. Biol. 262 (5), 652–670.

Grieco, F., Lanave, C., Gallitelli, D., 1997. Evolutionary dynamics of cucumber mosaic virus satellite RNA during natural epidemics in Italy. Virology 229 (1), 166–174.

Hall, J.S., French, R., Morris, T.J., Stenger, D.C., 2001. Structure and temporal dynamics of populations within wheat streak mosaic virus isolates. J. Virol. 75 (21), 10231–10243.

Hofacker, I.L., Stadler, P.F., Stocsits, R.R., 2004. Conserved RNA secondary structures in viral genomes: a survey. Bioinformatics 20 (10), 1495–1499.

Hsu, Y.H., Lee, Y.S., Liu, J.S., Lin, N.S., 1998. Differential interactions of bamboo mosaic potexvirus satellite RNAs, helper virus, and host plants. Mol. Plant Microbe Interact. 11, 1207–1213.

Huang, C.Y., Huang, Y.L., Meng, M., Hsu, Y.H., Tsai, C.H., 2001. Sequences at the 3′ untranslated region of bamboo mosaic potexvirus RNA interact with the viral RNA-dependent RNA polymerase. J. Virol. 75 (6), 2818–2824.

Kumar, S., Tamura, K., Jakobsen, I.B., Nei, M., 2001. MEGA2: molecular evolutionary genetics analysis software. Bioinformatics 17 (12), 1244–1245.

Kurath, G., Heick, J.A., Dodds, J.A., 1993. RNase protection analyses show high genetic diversity among field isolates of satellite tobacco mosaic virus. Virology 194 (1), 414–418.

Kurosaki, M., Enomoto, N., Nouchi, T., Sakuma, I., Marumo, F., Sato, C., 1995. Fraction-specific populations of the hypervariable region of the hepatitis C virus in a patient with cryoglobulinemia. J. Med. Virol. 46 (4), 403–408.

Leitmeyer, K.C., Vaughn, D.W., Watts, D.M., Salas, R., Villalobos, I., de Chacon, C., Rico-Hesse, R., 1999. Dengue virus structural differences that correlate with pathogenesis. J. Virol. 73 (6), 4738–4747.

Li, W.H., 1993. Unbiased estimation of the rates of synonymous and nonsynonymous substitution. J. Mol. Evol. 36 (1), 96–99.

Li, Y.I., Cheng, Y.M., Huang, Y.L., Tsai, C.H., Hsu, Y.H., Meng, M., 1998. Identification and characterization of the *Escherichia coli*-expressed RNA-dependent RNA polymerase of bamboo mosaic virus. J. Virol. 72 (12), 10093–10099.

Li, Y.I., Shih, T.W., Hsu, Y.H., Han, Y.T., Huang, Y.L., Meng, M., 2001. The helicase-like domain of plant potexvirus replicase participates in formation of RNA 5′ cap structure by exhibiting RNA 5′-triphosphatase activity. J. Virol. 75 (24), 12114–12120.

Lin, N.S., Chen, C.C., 1991. Association of Bamboo mosaic virus (BaMV) and BaMV-specific electron-dense crystalline bodies with chloroplasts. Phytopathology 81, 1551–1555.

Lin, N.S., Hsu, Y.H., 1994. A satellite RNA associated with bamboo mosaic potexvirus. Virology 202 (2), 707–714.

Lin, N.S., Chai, Y.J., Huang, T.Y., Chang, T.Y., Hsu, Y.H., 1993. Incidence of bamboo mosaic potexvirus in Taiwan. Plant Dis. 77, 448–450.

Lin, N.S., Lin, B.Y., Lo, N.W., Hu, C.C., Chow, T.Y., Hsu, Y.H., 1994. Nucleotide sequence of the genomic RNA of bamboo mosaic potexvirus. J. Gen. Virol. 75 (Pt. 9), 2513–2518.

Lin, N.S., Lee, Y.S., Lin, B.Y., Lee, C.W., Hsu, Y.H., 1996. The open reading frame of bamboo mosaic potexvirus satellite RNA is not essential for its replication and can be replaced with a bacterial gene. Proc. Natl. Acad. Sci. U.S.A. 93 (7), 3138–3142.

Lin, M.K., Chang, B.Y., Liao, J.T., Lin, N.S., Hsu, Y.H., 2004. Arg-16 and Arg-21 in the N-terminal region of the triple-gene-block protein 1 of Bamboo mosaic virus are essential for virus movement. J. Gen. Virol. 85 (Pt. 1), 251–259.

Liu, J.S., Lin, N.S., 1995. Satellite RNA associated with bamboo mosaic potexvirus shares similarity with satellites associated with sobemoviruses. Arch. Virol. 140 (8), 1511–1514.

Liu, J.S., Hsu, Y.H., Huang, T.Y., Lin, N.S., 1997. Molecular evolution and phylogeny of satellite RNA associated with bamboo mosaic potexvirus. J. Mol. Evol. 44 (2), 207–213.

Pamilo, P., Bianchi, N.O., 1993. Evolution of the Zfx and Zfy genes: rates and interdependence between the genes. Mol. Biol. Evol. 10 (2), 271–281.

Palukaitis, P., Roossinck, M.J., 1995. Variation in the hypervariable region of cucumber mosaic virus satellite RNAs is affected by the helper virus and the initial sequence context. Virology 206 (1), 765–768.

Pelchat, M., Levesque, D., Ouellet, J., Laurendeau, S., Levesque, S., Lehoux, J., Thompson, D.A., Eastwell, K.C., Skrzeczkowski, L.J., Perreault, J.P., 2000. Sequencing of peach latent mosaic viroid variants from nine North American peach cultivars shows that this

RNA folds into a complex secondary structure. Virology 271 (1), 37–45.
Pinel, A., Abubakar, Z., Traore, O., Konate, G., Fargette, D., 2003. Molecular epidemiology of the RNA satellite of Rice yellow mottle virus in Africa. Arch. Virol. 148 (9), 1721–1733.
Polivka, H., Staub, U., Gross, H.J., 1996. Variation of viroid profiles in individual grapevine plants: novel grapevine yellow speckle viroid 1 mutants show alterations of hairpin I. J. Gen. Virol. 77 (Pt. 1), 155–161.
Roossinck, M.J., 2002. Evolutionary history of Cucumber mosaic virus deduced by phylogenetic analyses. J. Virol. 76 (7), 3382–3387.
Roossinck, M.J., Sleat, D., Palukaitis, P., 1992. Satellite RNAs of plant viruses: structures and biological effects. Microbiol. Rev. 56, 265–279.
SAS Institute, 2001. PROC User's Manual, Version 6th ed. SAS Institute, Cary, NC.
Schneider, W.L., Roossinck, M.J., 2000. Evolutionarily related Sindbis-like plant viruses maintain different levels of population diversity in a common host. J. Virol. 74 (7), 3130–3134.
Schuster, P., Fontana, W., Stadler, P.F., Hofacker, I.L., 1994. From sequences to shapes and back: a case study in RNA secondary structures. Proc. R. Soc. Lond., B Biol. Sci. 255 (1344), 279–284.
Shurtleff, A.C., Beasley, D.W.C., Chen, J.J.Y., Ni, H., Suderman, M.T., Wang, H., Xu, R., Wang, E., Weaver, S.C., Watts, D.M., Russell, K.L., Barrett, D.T., 2001. Genetic variation in the 3′ non-coding region of dengue viruses. Virology 281, 75–87.
Simon, A.E., 1999. Replication, recombination, and symptom-modulation properties of the satellite RNAs of turnip crinkle virus. Curr. Top. Microbiol. Immunol. 239, 19–36.
Simon, A.E., Roossinck, M.J., Havelda, Z., 2004. Plant virus satellite and defective interfering RNAs: new paradigms for a new century. Annu. Rev. Phytopathol. 42, 415–437.
Sumi, S., Matsumi, T., Tsuneyoshi, T., 1999. Complete nucleotide sequences of garlic viruses A and C, members of the newly ratified genus Allexivirus. Arch. Virol. 144 (9), 1819–1826.
Tsai, C.H., Cheng, C.P., Peng, C.W., Lin, B.Y., Lin, N.S., Hsu, Y.H., 1999. Sufficient length of a poly(A) tail for the formation of a potential pseudoknot is required for efficient replication of bamboo mosaic potexvirus RNA. J. Virol. 73 (4), 2703–2709.
Tsai, M.S., Hsu, Y.H., Lin, N.S., 1999. Bamboo mosaic potexvirus satellite RNA (satBaMV RNA)-encoded P20 protein preferentially binds to satBaMV RNA. J. Virol. 73 (4), 3032–3039.
Vogt, P.K., Jackson, A.O., 1999. Satellites and Defective Viral RNAs. Springer, Berlin.
White, K.A., Bancroft, J.B., Mackie, G.A., 1992. Mutagenesis of a hexanucleotide sequence conserved in potexvirus RNAs. Virology 189 (2), 817–820.
Wung, C.H., Hsu, Y.H., Liou, D.Y., Huang, W.C., Lin, N.S., Chang, B.Y., 1999. Identification of the RNA-binding sites of the triple gene block protein 1 of bamboo mosaic potexvirus. J. Gen. Virol. 80 (Pt. 5), 1119–1126.
Yang, C.C., Liu, J.S., Lin, C.P., Lin, N.S., 1997. Nucleotide sequence and phylogenetic analysis of a bamboo mosaic potexvirus isolate from common bamboo (*Bambusa vulgaris* McClure). Bot. Bull. Acad. Sin. 38, 77–84.
Zuker, M., Matthews, D.H., Turner, D.H., 1999. Algorithms and thermodynamics for RNA secondary structure prediction: a practical guide. In: Barciszewski, J., Clark, B.F.C. (Eds.), RNA Biochemistry and Biotechnology NATO ASI Series. Kluwer Academic Publishers, Dordrecht, Netherlands, pp. 11–43.